ELSEVIER

Journal of Molecular Catalysis A: Chemical 151 (2000) 147–160

JOURNAL OF MOLECULAR CATALYSIS A: CHEMICAL

www.elsevier.com/locate/molcata

Lewis base adducts of bis-(halogeno)dioxomolybdenum(VI): syntheses, structures, and catalytic applications

Fritz E. Kühn [a,*], André D. Lopes [b], Ana M. Santos [a], Eberhardt Herdtweck [a], Joachim J. Haider [a], Carlos C. Romão [b], A. Gil Santos [c]

[a] *Anorganisch-chemisches Institut der Technischen Universität München, Lichtenbergstraße 4, D-85747 Garching bei München, Germany*
[b] *Instituto de Tecnologia Química e Biológica da Universidade Nova de Lisboa, Quinta do Marquês, EAN, Apartado 127, P-2781-901 Oeiras, Portugal*
[c] *Departamento de Química, Centro de Química Fina e Biotecnologia, Faculdade de Ciências e Tecnologia, Universidade Nova de Lisboa, P-2825 Monte de Caparica, Portugal*

Received 15 April 1999; received in revised form 25 May 1999; accepted 22 June 1999

Abstract

Reaction of solvent substituted $MoO_2X_2(Solv)_2$ complexes ((Solv) = THF, CH_3CN) with mono- and bidentate nitrogen and oxygen donor ligands leads to complexes of the type $MoO_2X_2L_2$ in nearly quantitative yields at room temperature within a few minutes. The ^{95}Mo and ^{17}O NMR data of selected complexes as well as the Mo=O IR vibrations were used to probe the influence of the ligands on the electronic properties of the metal and the Mo=O bond. Two complexes have additionally been examined by single crystal X-ray analysis. The activity of the $MoO_2X_2L_2$ complexes as catalysts in olefin epoxidation with *t*-butylhydroperoxide as oxidizing agent depends on both the nature of the organic ligand L and the halogeno ligand X. The difference in activity observed between Cl and Br substituted complexes is not very pronounced. In general, the Cl derivatives are more active than their Br analogues. The organic ligands L display a significant influence on the catalytic performance. Complexes with ligands bearing aromatic substituents at N are in all cases, much more active than those bearing aliphatic substituents. The less active complexes can be activated by raising the temperature and extending the reaction time. In all observed cases, these changes produce a significant increase of the product yield.

Keywords: Catalysis; Chelating ligands; Molybdenum; Olefins; Oxidation; X-ray structures

1. Introduction

Several molybdenum(VI) complexes have proven to be useful catalysts for the epoxidation of olefins with hydroperoxides like H_2O_2 and alkylperoxides and the mechanism of these reactions has been recently reexamined [1–3]. With regard to the catalyst precursors, two types of complex are particularly important, namely the bisperoxo complexes **A** and the *cis*-MoO_2^{2+} derivatives **B**.

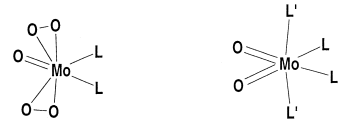

A B

* Corresponding author.

1381-1169/00/$ - see front matter
PII: S1381-1169(99)00262-9

Peroxomolybdenum compounds have been recently examined in great detail by the groups of Thiel and Priermeier [2], Thiel [3], Thiel and Eppinger [4], Ballisteri et al. [5] and Campestrini and di Furia [6]. In these complexes, the control of the activity can be achieved exclusively by varying the ligand L.

In the case of the *cis*-MoO_2^{2+} complexes, the general formula is MoO_2L_4 (or $MoO_2L_2L'_2$). Depending on the nature of the ligands, three main complex types have been examined in more detail for catalytic purposes, despite the fact that a much broader variety of compounds is known. The first dioxomolybdenum(VI) complex examined in epoxidation catalysis was the bis(acetylacetonato)dioxomolybdenum(VI), described by Indictor and Brill [7]. Aminoalcoholate complexes followed, leading to patents of the so-called ARCO-process [8–11]. Finally, Schiff-bases have been used as ligands of the $(Mo(VI)O_2)^{2+}$ moiety [12]. The acetylacetonato complexes and derivatives have been examined more often in epoxidation catalysis, due to their easy and straightforward synthesis [13,14].

Few catalytic studies of $MoO_2X_2L_2$ complexes have been carried out to date. The most important ones regard the complexes with non-chelating O donor ligands L and those with solvento complexes [15–19]. It has been shown that these systems form monoperoxo complexes in stoichiometric reactions with certain organoperoxides [18], but the reaction with excess peroxide has never been examined in detail. $MoO_2X_2L_2$ systems with chelating nitrogen ligands display two important advantages: first, the two different ligand sets X and L can be easily varied in order to fine tune the ligand surrounding of the Mo(VI) center. Secondly, bidentate nitrogen donor ligands offer a great versatility in modifying the electron donor and acceptor properties of the ligands L.

In the present study, $MoO_2X_2L_2$-type (X = Cl, Br) complexes were prepared from the solvent adducts of the halogenated molybdenum oxides and a variety of substituted 1,4-diazabutadienes (R-DAB) (R = *i*-propyl, *t*-butyl, cyclohexyl, *o*-tolyl, *p*-tolyl) ligands and the related *N,N*-dicyclohexyl-2,3-dimethyl-1,4-diazabutadiene. These ligands were chosen considering their good coordination capabilities. For comparison purposes, complexes with non-chelating organic oxygen donor ligands were also prepared with picoline *N*-oxide, acac(acac$^-$ = acetylacetonate) related ligands, 4-anilino-pent-3-ene-2-one, $CH_3C(O)CHC(N(H)Ph)CH_3$, and 4-methylamino-pent-3-ene-2-one [$CH_3C(O)$-$CHC(N(H)CH_3]CH_3$]. These complexes were characterized and their behavior as olefin epoxidation catalysts with *t*-butylhydroperoxide as oxidant was studied.

2. Results and discussion

*2.1. Synthesis and spectroscopic examinations of compounds **1–20***

Organic ligands with donor functionalities such as nitrogen or oxygen atoms react readily with complexes of the type $MoO_2X_2(Solv)_2$ (X = Cl, Br; (Solv) = THF, $NCCH_3$) forming the octahedrally coordinated complexes **1–20** (Eq. 1)

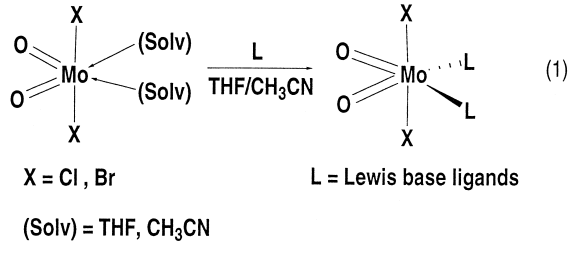

(1)

at room temperature within minutes (Fig. 1). The product complexes are in general significantly less soluble than the starting materials and precipitate from the reaction mixture. They can be purified (e.g., from excess of ligand) by washing with diethyl ether and pentanes or hexanes.

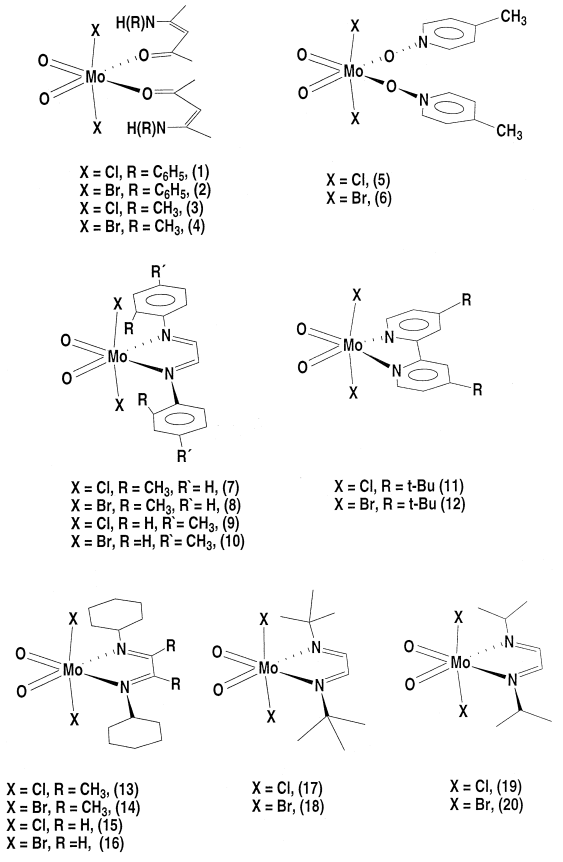

Fig. 1. Formulae of the complexes synthesized in this work according to Eq. 1.

The complexes **1**–**6**, bearing non-chelating oxygen organic ligands decompose within a few hours when exposed to air. The chelating nitrogen ligand complexes **7**–**20** are in general more stable. Several of them are fully stable under laboratory atmosphere and all of them can be handled in air. This represents a remarkable difference to the acetonitrile or THF substituted starting materials, which are both air- and moisture sensitive and can only be handled and stored under moisture-free inert gas atmosphere. The better donor capabilities and perhaps also, the greater steric bulk of the chelating product complexes **7**–**20**, stabilize these molecules significantly. The mixed N,O ligands of the β-ketoimine type act as monodentate and coordinate via the O atom, as demonstrated crystallographically for **3** (see below). The complexes MoO_2X_2(^{t}Bubipy) (X = Cl (**11**), Br (**12**)) and MoO_2X_2-(^{t}Bu-DAB) (**17**), have been already mentioned in the literature [20–22].

Most of the complexes **1**–**20** are soluble enough in polar organic solvents to produce ^{1}H NMR spectra of sufficient quality. However, the chemical shifts of the protons of these compounds do not differ significantly from those of the free organic ligands.

^{95}Mo NMR spectra of the more soluble complexes are shown in Table 1. Unfortunately, several of the synthesized compounds **1**–**20** are not soluble enough to give ^{95}Mo NMR spectra of sufficient quality. The ^{95}Mo NMR spectra display their signals in the region between ca. 190 and 280 ppm, the same found for the starting complex $MoO_2Br_2(NCCH_3)_2$, which displays its ^{95}Mo signal at $\delta(^{95}\text{Mo}) = 278$ ppm. Solvent effects have not been observed: in all cases examined, the chemical shift of a given complex in different solvents (e.g., methylene chloride or toluene vs. THF or CH_3CN) differs less then 5 ppm. This observation indicates that the ligand surrounding of the Mo(VI) center is not significantly influenced by the solvent. The ^{95}Mo NMR spectra of the product complexes show a higher shielding of this nucleus as compared to the solvent coordinated starting materials. Despite the fact that the generally low solubility of the synthesized complexes has hampered a more thorough study of the ligand influence on the chemical shift of this system by

Table 1
^{95}Mo and ^{17}O NMR (terminal oxoligands) data of selected complexes. CH_2Cl_2, CH_3CN and toluene, respectively, were used as solvents

Compound	Chemical shift (ppm)	Compound	Chemical shift (ppm)
3	$\delta(^{95}\text{Mo}) = 160$	**1**	$\delta(^{17}\text{O}) = 961$
4	$\delta(^{95}\text{Mo}) = 192$	**2**	$\delta(^{17}\text{O}) = 936$
5	$\delta(^{95}\text{Mo}) = 189$	**3**	$\delta(^{17}\text{O}) = 970$
6	$\delta(^{95}\text{Mo}) = 220$	**4**	$\delta(^{17}\text{O}) = 927$
13	$\delta(^{95}\text{Mo}) = 221$		
17	$\delta(^{95}\text{Mo}) = 216$		
18	$\delta(^{95}\text{Mo}) = 277$		
19	$\delta(^{95}\text{Mo}) = 207$		
20	$\delta(^{95}\text{Mo}) = 265$		

^{95}Mo NMR, some conclusions may still be drawn.

There is a clear inverse halogen dependence on the chemical shift of the ^{95}Mo NMR spectra since the signals of the chloro complexes (**5**, **17**, **19**) are observed at higher field than those of the bromo derivatives (**6**, **18**, **20**) (Table 1). The $\delta(^{95}\text{Mo})$ shift difference between the Cl and the Br complexes lies between 30 and 60 ppm in the examined cases. Such an inverse halogen dependence has been observed in other few cases, which include other Mo(VI) derivatives of the MoO_2^{2+} core [23].

The ^{95}Mo NMR signals of the complexes with monodentate oxygen ligands (**3**–**6**) are shifted to higher field compared to the complexes with N donor ligands (**13**, **17**–**20**) regardless of their denticity. Given the high sensitivity of the ^{95}Mo chemical shift, it is interesting to note the similarity of the chemical shifts among complexes with N-substituted 1,3-DAB ligands (**13**, **17**, **19**). It demonstrates that different R groups in the DAB ligand do not strongly influence the electron density at the metal center of these complexes. The half widths of all examined complexes are below 100 Hz and therefore, comparatively narrow, not indicating special ligand exchange phenomena or equilibria between different species. Temperature changes do not lead to significant changes of the half widths of the signals.

The precursor compound $MoO_2Br_2(NCCH_3)_2$ displays its ^{17}O NMR signal at $\delta(^{17}\text{O}) = 1024$ ppm. The chemical shifts of the terminal oxygen atoms measured for the sufficiently soluble complexes (see Table 1) are in the expected range for transition metal oxo complexes in high oxidation states [24,25], namely between 900 and 1000 ppm. The half width of the observed signals is ca. 50 Hz. It seems that the O atoms of the Br containing compounds are more deshielded than those of the Cl substituted derivatives. We examined both the oxygen and the organic ligand exchange with ^{17}O marked methyltrioxorhenium(VII), which is known to exchange easily its oxo functionalities with other transition metal oxo complexes e.g., OsO_4 [26]. It is also known that donor adducts of organorhenium(VII) oxides, $RReO_3L_n$, readily exchange Lewis base ligands, especially in donor solvents at room temperature and above [26,27]. However, in our experiments, we did not observe any significant ligand exchange between complexes substituted with nitrogen donor ligands such as **7** and methyltrioxorhenium(VII) (Scheme 1) even after several hours in toluene at 90°C. In the case of oxygen donor derivatives such as **1**–**6** oxygen exchange with ^{17}O labelled $CH_3Re^{17}O_3$ occurred after about 2 h reaction time in toluene at 90°C to a minor but detectable degree. Unlabelled complexes measured under comparable conditions did not give rise to detectable ^{17}O NMR signals. However, we did not find any indication for the exchange of the organic donor ligands between the Mo and the Re complexes. In the Mo case, both oxygen and nitrogen atoms of the organic ligands seem to be bound more strongly. An oxygen ligand exchange does also not occur easily. This could be interpreted in terms of the coordinative saturation of the Mo(VI) center by the strongly coordinated organic ligands. The formation of oxygen bridges, which are suspected

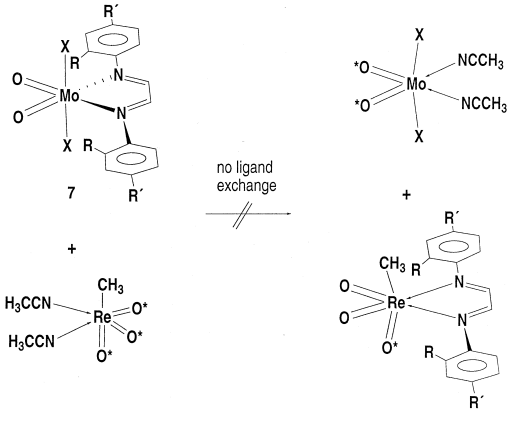

Scheme 1. Neither exchange of terminal oxygens nor that of the N-donor ligands between $MoO_2X_2L_2$ and CH_3ReO_3 can be observed.

to be responsible for the exchange mechanism is therefore, seemingly hindered.

The complexes **1**–**20** display their Mo=O stretching vibrations in the expected range [28]. The symmetric and unsymmetric vibrations are observed at ca. 935 and 905 cm^{-1}, varying ca. ± 10 cm^{-1}. Within the experimental error of the measurement itself (± 4 cm^{-1}), the vibrations are all very similar. The IR data also support the fact that the complexes **1**–**20** display a distorted octahedral C_{2v}-geometry (see X-ray section) with the oxygen atoms in *trans* position to the organic donor ligand(s) in the equatorial plane and the halogeno atoms in *trans* position to each other in the apical positions.

2.2. X-ray crystallography

The molecular structure of the compounds **3** and **5** · $NCCH_3$ was determined by X-ray crystallography. Details of the single crystal X-ray experiments are given in Table 2. Key bond distances are listed in Table 3. Both compounds (Figs. 2 and 3) are monomeric. The core geome-

Table 2
Crystallographic data for $MoO_2Cl_2[CH_3C(O)CHC(N(H)CH_3)CH_3]_2$ (**3**), and MoO_2Cl_2(pic.*N*-oxide)$_2$ · $NCCH_3$(**5** · $NCCH_3$)

	3	**5**
Chemical formula	$C_{12}H_{22}Cl_2MoN_2O_4$	$C_{12}H_{14}Cl_2MoN_2O_4 \cdot NCCH_3$
fw	425.16	458.15
Color/shape	yellow/fragment	yellow/fragment
Cryst. size (mm)	0.38 · 0.25 · 0.20	0.66 · 0.56 · 0.46
Cryst. system	monoclinic	monoclinic
Space group	C2/c	$P2_1/n$
a (pm)	838.1(1)	1113.1(1)
b (pm)	1657.0(2)	1400.3(1)
c (pm)	1258.0(2)	1197.7(1)
α (°)	90	90
β (°)	93.20(1)	95.59(1)
γ (°)	90	90
V (10^6 pm^3)	1744.3(4)	1857.9(3)
Z	4	4
T (K)	193	193
$\rho_{calcd.}$ ($g\ cm^{-3}$)	1.619	1.638
μ (mm^{-1})	1.07	1.02
F_{000}	864	920
λ (pm)	71.073	71.073
Device/scan method	IPDS/ϕ-rotation	IPDS/ϕ-rotation
Θ-range (°)	2.73 to 24.81	3.68 to 30.38
Data collected (*h*,*k*,*l*)	± 9, ± 19, ± 14	± 15, ± 19, ± 16
Number of reflections collected	10,624	39,186
Number of independent reflections	1473	4448
Number of observed reflections	1473 (all data)	4448 (all data)
Number of parameters refined	140	291
R_{int}	0.0209	0.0399
R1[a]	0.0257	0.0313
wR2[b]	0.0700	0.0743
GOF[c]	1.153	1.069
Weights *a*/*b*[d]	0.0408/3.03	0.0369/1.39
$\Delta\rho_{max/min}$ (e $Å^{-3}$)	+0.27/−0.43	+0.45/−0.50

[a] $R1 = \Sigma(||F_o| - |F_c||)/\Sigma|F_o|$.
[b] $wR2 = [\Sigma w(F_o^2 - F_c^2)^2/\Sigma w(F_o^2)^2]^{1/2}$.
[c] $GOF = [\Sigma w(F_o^2 - F_c^2)^2/(NO - NV)]^{1/2}$.
[d] $w \equiv 1/[\sigma^2(F_o^2) + (a \cdot P)^2 + b \cdot P]$ with P: [max(0 or F_o^2) + $2F_c^2$]/3.

try around the molybdenum atom is best described as a distorted octahedron with two chloride atoms *trans* to each other, two oxygen atoms and two N/O-ligands in a *cis* position The Mo–Cl, Mo=O, and the Mo–O/N bond distances are in good accordance with data reported in the literature for analogous compounds of the $MoCl_2O_2L_2$ type [29].

Table 3
Selected interatomic distances (pm) and angles (°) for $MoO_2Cl_2[CH_3C(O)CHC(N(H)CH_3)CH_3]_2$ (**3**), and MoO_2Cl_2(pic.*N*-oxide)$_2\cdot NCCH_3$ (**5**)

3		**5**$\cdot NCCH_3$	
Mo–Cl	238.81(8)	Mo–Cl(1)	240.33(6)
		Mo–Cl(2)	238.54(6)
Mo–O(1)	218.29(19)	Mo–O(1)	218.87(15)
		Mo–O(2)	216.55(14)
Mo–O(2)	168.78(19)	Mo–O(3)	169.86(15)
		Mo–O(4)	168.72(19)
O(1)–C(2)	128.3(3)	O(1)–N(11)	134.1(2)
N–C(4)	131.7(4)	O(2)–N(21)	134.9(2)
N–C(6)	144.5(5)	N(11)–C(12)	134.6(3)
C(1)–C(2)	149.6(5)	N(11)–C(16)	134.4(3)
C(2)–C(3)	138.7(5)	N(21)–C(22)	134.0(3)
C(3)–C(4)	139.7(4)	N(21)–C(26)	133.8(3)
C(4)–C(5)	149.9(5)	C(12)–C(13)	136.8(3)
		C(13)–C(14)	138.9(3)
		C(14)–C(15)	138.6(3)
		C(14)–C(17)	149.9(3)
		C(15)–C(16)	137.0(4)
		C(22)–C(23)	136.8(3)
		C(23)–C(24)	138.8(3)
		C(24)–C(25)	138.1(3)
		C(24)–C(27)	150.6(3)
		C(25)–C(26)	138.1(3)
Cl–Mo–O(1)	82.38(5)	Cl(1)–Mo–O(2)	81.99(4)
Cl–Mo–O(2)	95.46(6)	Cl(1)–Mo–O(3)	95.93(5)
Cl–Mo–Cl_a	161.76(3)	Cl(1)–Mo–Cl(2)	164.13(3)
Cl–Mo–O(1)a	83.02(5)	Cl(1)–Mo–O(1)	84.77(4)
Cl–Mo–O(2)a	95.96(6)	Cl(1)–Mo–O(4)	92.12(8)
O(1)–Mo–O(2)	92.15(8)	O(2)–Mo–O(3)	87.61(6)
Cl_a–Mo–O(1)	83.02(5)	Cl(2)–Mo–O(2)	86.08(4)
O(1)–Mo–O(1)a	73.45(7)	O(1)–Mo–O(2)	78.57(5)
O(1)–Mo–O(2)a	165.60(8)	O(2)–Mo–O(4)	167.76(7)
Cl_a–Mo–O(2)	95.96(6)	Cl(2)–Mo–O(3)	93.99(5)
O(1)a–Mo–O(2)	165.60(8)	O(1)–Mo–O(3)	165.94(7)
O(2)–Mo–O(2)a	102.25(9)	O(3)–Mo–O(4)	103.72(8)
Cl_a–Mo–O(1)a	82.38(5)	Cl(2)–Mo–O(1)	82.63(4)
Cl_a–Mo–O(2)a	95.46(6)	Cl(2)–Mo–O(4)	97.54(8)
O(1)a–Mo–O(2)a	92.15(8)	O(1)–Mo–O(4)	90.26(7)
Mo–O(1)–C(2)	142.63(19)	Mo–O(1)–N(11)	123.13(11)
		Mo–O(2)–N(21)	124.73(11)

Symmetry operation O → O_a: $(-x, y, 0.5-z)$.

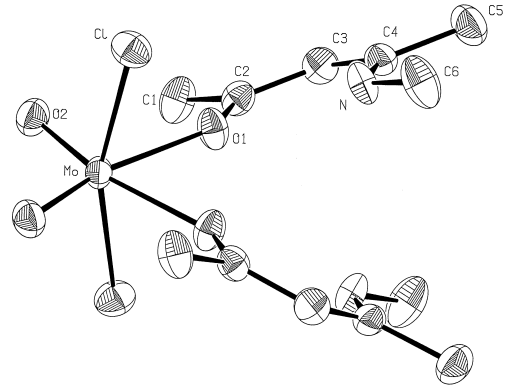

Fig. 2. ORTEP style plot of (**3**) with the atomic labelling scheme. Thermal ellipsoids are drawn at the 50% probability level. Hydrogen atoms are omitted for clarity. The molecule has C_2-symmetry with the two-fold axis bisecting the O1–Mo–O1a angle.

2.3. $MoO_2X_2L_2$ complexes in oxidation catalysis

We examined most of the complexes described above in the catalytic oxidation of cyclooctene with *t*-butylhydroperoxide. The broad variety of ligands enabled us to do a systematic study on the influence of the ligands on the catalytic performance of the catalysts. We additionally wanted to compare the catalytic behavior of chloride and bromide substituents in otherwise identical molecules. The experimental

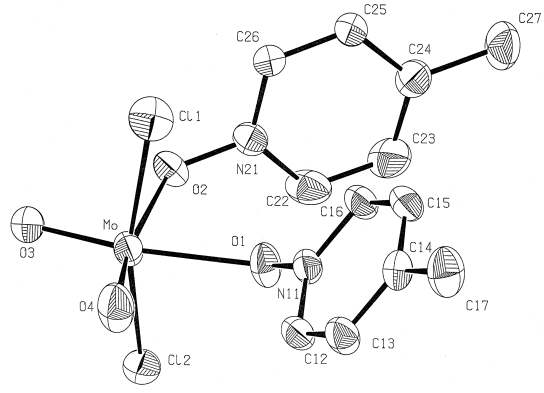

Fig. 3. ORTEP style plot of (**5**$\cdot NCCH_3$) with the atomic labelling scheme. Thermal ellipsoids are drawn at the 50% probability level. Hydrogen atoms are omitted for clarity.

details are given in the experimental part. Blank reactions have been performed and, as expected, it turned out that without catalyst, no significant epoxide formation was observed under any of the applied conditions. Significant byproduct formation e.g., diol instead of epoxide, was never observed either in the uncatalysed or catalysed runs. The oxidizing agent was only consumed during the epoxidation process of the olefin. A typical catalytic run is shown in Fig. 4 for the efficient catalyst MoO_2Cl_2(*o*-tolyl-DAB) (**7**). The reaction reaches a conversion of ca. 90% after about 4 h. Running the reaction 24 h does not significantly improve the yield (Fig. 5). Compounds showing a worse catalytic performance than compound **7** within 4 h usually display a significant increase of product formation within 24 h as can also be seen in Fig. 5. This indicates that the low yield after 4 h is not mainly due to decomposition of the particular catalyst under the applied reaction conditions but to a sluggish reaction. This activity is of the same order of magnitude of the activity of more common Mo catalysts like $Mo(CO)_6$ and $MoO_2(acac)_2$ (Fig. 5).

The influence of the ratio of oxidant to olefin was examined for compound **11**. The conversion raises with this ratio and after 4 h reaction time (55°C) 43%, 53% and 60% yields are achieved for a 1:1, 1:1.5 and 1:2 ratio, respectively. After 24 h, these yields increase to 67%, 70% and 72%, respectively.

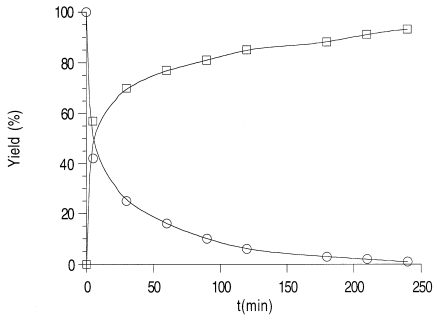

Fig. 4. Catalytic activity of $MoCl_2O_2$(*o*-phenyl-DAB) (**7**) in the presence of TBHP in the catalytic epoxidation of cyclooctene epoxidation. See text and Section 4 for reaction details.

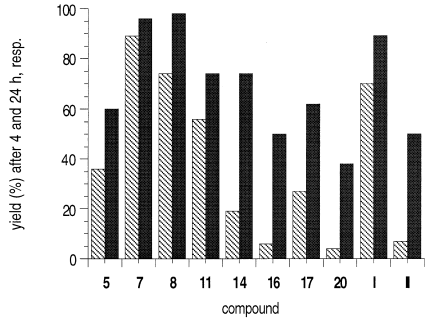

Fig. 5. Yield of cyclooctene epoxide in the presence of selected epoxidation catalysts after 4 and 24 h, respectively (Compound **I** = Mo_2O_2(acac), **II** = $Mo(CO)_6$).

A considerable influence of the coordinating ligands on the product yield can be observed. A first general observation clearly seen in Fig. 6 is the higher catalytic activity of the chloro complexes in comparison to the bromo analogues e.g., **5** vs. **6** or **7** vs. **8**. It is also obvious that the complexes containing ligands with aromatic substituents are more active than those with ligands containing aliphatic substituents in identical positions e.g., **7** vs. **17**. However, the yield difference between chlorinated and brominated complexes is in general considerably smaller than the differences caused by the changes of the organic ligand. This shows that activity growth correlates with electron density at the metal: electron attracting ligands improve activity. Furthermore, this fact suggests that the organic ligands remain attached to the metal in the catalytic active center and determine its activity.

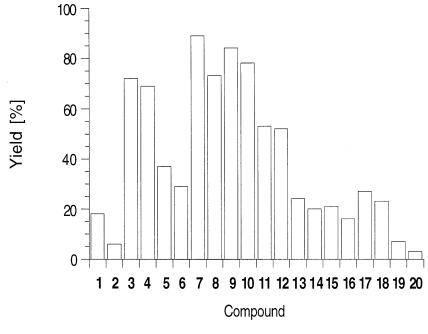

Fig. 6. Yield of cyclooctene epoxide in the presence of compounds **1**–**20** as catalysts after 4 h reaction time. See text and Section 4 for reaction details.

Of course, we cannot rule out that the true catalytic activity is due to another species derived from our precursor complexes. In order to establish the number and eventually the nature of the Mo complexes present in solution under catalytic conditions, we tried to follow the course of the reaction by ^{95}Mo and ^{1}H NMR. Unfortunately, the rather limited solubility of these Mo catalysts or catalyst precursors prevented the observation of any ^{95}Mo resonance at 55°C or even higher temperatures and no significant changes were detected in the resonances of the ligand protons. This at least shows that no significant oxidation or liberation of the ligands took place under the reaction conditions applied. Steric hindrance does not seem to play an important role as the activity of complexes **7**–**10** are similar as well as the activity of **13**–**20**.

Another point worth mentioning is the behavior of the complexes at higher and lower temperatures as depicted in Fig. 7 with the medium active complex **11** as an example. The higher the temperature, at least within the examined range between 25 and 90°C, the higher the product yield. This statement seems to be trivial on the first glance but several examples are known where the catalytic activity of oxidation catalysts decreases with increasing temperature above a certain level e.g., in the case of CH_3ReO_3 [30] and $(CH_3)_2MoO_2L_2$ [31]. It is also important to notice that the conversion without catalyst at 90°C is considerably lower than the conversion with catalyst at 25°C.

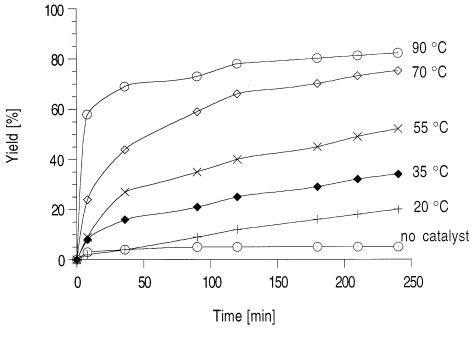

Fig. 7. Temperature dependence of the catalytic activity of compound **11**. A run without catalyst at 90°C reaction temperature is shown for comparison.

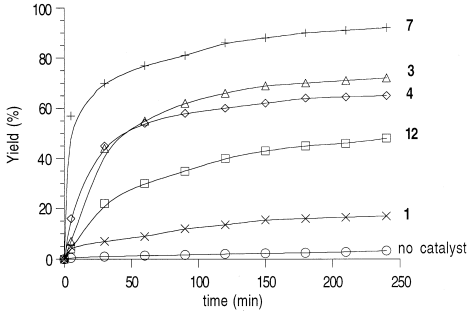

Fig. 8. Time-dependent yield of cyclooctene epoxide in the presence of selected oxidation catalysts at 55°C. A run without catalyst at 55°C is shown for comparison.

All catalytic reactions show the same time-dependent curve form (Fig. 8). After a quick increase of the yield within the first hour the reaction velocity slows down. The appearance of these curves does not indicate the transformation of the original catalyst in another species during the reaction time and does not show an observable induction period. According to the related examples in the literature, the active species may be an alkylperoxo complex [2,3] or a peroxo complex in which case, it may be either a monoperoxo or a bisperoxo complex [18]. In the present case, all attempts to identify the nature of the active peroxo species were thwarted by the low solubility of the complexes. Further work designed to overcome this limitation and help clarifying the nature of the active species of these reactions is currently under way in our laboratories.

3. Conclusions

A range of 1,3-diazabutadiene derivatives of MoO_2X_2 (X = Cl, Br) has been prepared and characterized by IR as well as ^{95}Mo and ^{17}O NMR spectroscopy. In spite of the similar spectroscopic properties of all these complexes, considerable activity differences have been found in the catalytic epoxidation of cyclooctene with *t*-butylhydroperoxide. The stability of the complexes and the ligand dependence observed suggest that these chelating ligands remain bound

to the active center throughout the reaction. This suggestion raises the possibility of achieving enantioselective oxidations by means of the appropriate chiral ligands. This possibility together with the study of the nature of the active species is currently under investigation in our laboratories.

4. Experimental section

All preparations and manipulations were done with standard Schlenk techniques under an atmosphere of nitrogen. Solvents were dried by standard procedures (THF, *n*-hexane and Et_2O over Na/benzophenone ketyl; CH_2Cl_2 and NCMe over CaH_2), distilled under argon and kept over 4 Å molecular sieves (3 Å for NCMe).

Microanalyses were performed at the ITQB. NMR spectra were measured on a Bruker CXP 300 and Bruker Avance DPX-400. ^1H NMR spectra were recorded at 300 MHz, ^{17}O NMR spectra were recorded at 54.14 MHz, ^{95}Mo NMR spectra at 26.07 MHz. The IR spectra were measured on a Unican Mattson Mod 7000 FTIR spectrometer. 4-Anilino-pent-3-ene-2-one [$CH_3C(O)CHC(HNPh)CH_3$] [32], 4-methylamino-pent-3-ene-2-one [$CH_3C(O)CHC(N(H)CH_3)CH_3$] [32], ^{t}Bubipy [33], CYDAB [34], *p*-phen.-DAB [35], *o*-phen.-DAB [36], Me-CYDAB [37], ^{t}Bu-DAB [38], iprop.-DAB [35], MoO_2Cl_2 [36], $MoO_2Cl_2(THF)_2$ [37], MoO_2Br_2 [36], $MoO_2Br_2(NC\text{-}Me)_2$ [38] were prepared as published or with minor changes. $MoO_2X_2 \cdot 2(THF)$ and $MoO_2X_2 \cdot 2(CH_3CN)$ were prepared as described [19].

4.1. $MoO_2Cl_2[CH_3C(O)CHC(N(H)Ph)CH_3]_2$ (1)

A solution of $MoO_2Cl_2(THF)_2$ (1.10 g, 3.20 mmol) in THF (15 ml), was treated with $CH_3C(O)CHC(HNCH_3)CH_3$ (0.72 g, 6.40 mmol). The colour of the solution changed to yellow and a yellow precipitate was formed. After 30 min, the suspension was brought to dryness to yield a yellow powder, which was washed with CH_2Cl_2 and diethyl ether. Yield: 87%.

$C_{12}H_{22}N_2O_4Cl_2Mo$ (425.17): calcd. C 48.10, H 5.10, N 4.77; found C 48.11, H 5.02, N 4.97. IR (KBr, υ (cm^{-1})): 3165 vs, 3094 vs, 3013 vs, 2971 vs, 2851 vs, 1611 vs, 1547 vs, 1492 vs, 1427 vs, 1364 vs, 1335 vs, 1316 vs, 1273 vs, 1209 vs, 1080 s, 936, 897, vs, υ(Mo=O), 835 s, 783 vs, 756 vs. ^1H NMR ($CHCl_3$-d_1, 300 MHz, r.t., δ (ppm)): 12.22 (b, 2H), 7.35–6.93 (m, 10H), 3.75 (s, 2H), 2.41 (s, 6H), 1.96 (s, 6H).

4.2. $MoO_2Br_2[_2CH_3C(O)CHC(N(H)Ph)CH_3]_2$ (2)

A solution of $MoO_2Br_2(NCMe)_2$ (0.47 g, 1.28 mmol) in THF (15 ml) was treated with $CH_3C(O)CHC(HNPh)CH_3$ (0.45 g, 2.56 mmol). The colour of the solution changed to orange and an orange precipitate was formed. The mixture reaction was stirred for 30 min and the suspension was then taken to dryness to yield an orange powder which was washed with CH_2Cl_2 and diethyl ether. Yield: 80%.

$C_{12}H_{22}N_2O_4Br_2Mo$ (526.10): calcd. C 41.40, H 4.11, N 4.39; found C 41.15, H 4.13, N 4.24. IR (KBr, υ (cm^{-1})): 3127 m, 3061 m, 2978 m, 1597 vs, 1580 vs, 1543 vs, 1495 vs, 1433 s, 1360 vs, 1339 vs, 1202 s, 937, 899, vs, υ(Mo=O), 756 vs, 694 s. ^1H NMR ($CHCl_3$-d_1, 300 MHz, r.t., δ (ppm)): 7.41–7.17 (m, 10H), 5.15 (b, 2H), 2.54 (s, 6H), 2.01 (s, 6H).

4.3. $MoO_2Cl_2[CH_3C(O)CHC(N(H)CH_3)CH_3]_2$ (3)

A solution of $MoO_2Cl_2(THF)_2$ (1.10 g, 3.20 mmol) in THF (15 ml), was treated with $CH_3C(O)CHC(HNCH_3)CH_3$ (0.72 g, 6.40 mmol). The initial light blue solution changed immediately to bright yellow and the mixture reaction was allowed to stir for further 30 min. The yellow turbid solution was taken to dryness to yield a yellow powder which was washed with CH_2Cl_2 and diethyl ether. Yield: 80%.

$C_{12}H_{22}N_2O_4Cl_2Mo$ (425.17): calcd. C 32.10, H 5.17, N 5.99; found: C 31.69; H 4.94; N 6.07. IR (KBr, υ (cm^{-1})): 3165 vs, 3094 vs, 3013 vs, 2971 vs, 2851 vs, 1611 vs, 1547 vs, 1492 vs, 1427 vs, 1364 vs, 1335 vs, 1316 vs, 1273 vs, 1209 vs, 1080 s, 936, 897, vs, υ(Mo=O), 835 s, 783 vs, 756 vs. ^{1}H NMR ($CHCl_3$-d_1, 300 MHz, r.t., δ (ppm)): 5.03 (b, 2H), 3.08 (s, 6H), 2.32 (s, 6H), 2.11 (s, 6H).

*4.4. $MoO_2Br_2[_2CH_3C(O)CHC(N(H)CH_3)CH_3]_2$ (**4**)*

A solution of $MoO_2Br_2(NCMe)_2$ (1.25 g, 3.39 mmol) in THF (15 ml) was treated with $CH_3C(O)CHC(HNCH_3)CH_3$ (0.77 g, 6.78 mmol). The colour of the solution became yellow and an orange precipitate appeared. After 30 min, the suspension was taken to dryness and the orange powder was washed with CH_2Cl_2 and diethyl ether. Yield: 80%.

$C_{12}H_{22}N_2O_4Br_2Mo$ (526.10): calcd. C 26.07, H 4.04, N 4.68; found: C 26.17, H 4.12, N 5.00. IR (KBr, υ (cm^{-1})): 3115 s, 2922 s, 1722 vs, 1613 vs, 1408 m, 1362 s, 1167 m, 1035 m, 957, 916, vs, υ(Mo=O), 866 s, 768 vs, 640 w, 571 s. ^{1}H NMR ($CHCl_3$-d_1, 300 MHz, r.t., δ (ppm)): 5.00 (b, 2H), 3.03 (s, 6H), 2.33 (s, 6H), 2.12 (s, 6H).

*4.5. MoO_2Cl_2(pic.N-oxide)$_2$ (**5**)*

A solution of $MoO_2Cl_2(THF)_2$ (1.21 g, 3.52 mmol) in THF (15 ml), was treated with picoline *N*-oxide (0.77 g, 7.04 mmol). The yellow/greenish turbid solution which formed was concentrated and the pale green product was precipitated by diethyl ether. Yield: 98%.

$C_{12}H_{14}N_2O_4Cl_2Mo$ (417.10): calcd: C 36.70, H 3.72, N 9.17; found C 36.69, H 3.72, N 9.16. IR (KBr, υ (cm^{-1})): 3123 s, 1626 s, 1493 vs, 1460 vs, 1209 vs, 1179 vs, 1121 s, 1040 m, 935, 903, vs, υ(Mo=O), 866 vs, 826 vs, 788 vs, 694 s. ^{1}H NMR ($CHCl_3$-d_1, 300 MHz, r.t., δ (ppm)): 8.62 (d, 4H), 7.40 (d, 4H), 2.50 (s, 6H).

*4.6. MoO_2Br_2(pic.N-oxide)$_2$ (**6**)*

A solution of $MoO_2Br_2(NCMe)_2$ (0.78 g, 2.11 mmol) in THF (15 ml) was treated with picoline *N*-oxide (0.46 g, 7.04 mmol). A yellow solution immediately formed. After concentration to ca. 3 ml and addition of diethyl ether, a crystalline yellow precipitate was obtained. The solid was filtered off, washed with diethyl ether and dried under vacuum. Yield: 98%.

$C_{12}H_{14}N_2O_4Br_2Mo$ (518.02): calcd. C 28.50, H 2.79, N 5.54; found C 28.55, H 2.79, N 5.46. IR (KBr, υ (cm^{-1})): 3103 s, 3046 m, 1628 m, 1499 vs, 1458 s, 1213 vs, 939, 906, vs, υ(Mo=O), 858 vs, 828 s, 770 vs, 579 w. ^{1}H NMR ($CHCl_3$-d_1, 300 MHz, r.t., δ (ppm)): 8.70 (s, 4H), 7.42 (d, 4H), 2.48 (s, 6H).

*4.7. MoO_2Cl_2(o-phenyl-DAB) (**7**)*

A solution of $MoO_2Cl_2(THF)_2$ (0.42 g, 1.23 mmol) in THF (15 ml), was treated with *o*-phenyl-DAB (0.29 g, 1.23 mmol). The slightly blue solution immediately changed to bright yellow and the reaction was stirred for further 30 min. The solution was taken to dryness and the yellowish red product was washed with diethyl ether and dried under vacuum. Yield: 94%.

$C_{16}H_{16}N_2O_2Cl_2Mo$ (435.16): calcd. C 44.16, H 3.71, N 6.44; found C43.95, H 3.94, N 6.74. IR (KBr, υ (cm^{-1})): 3023 w, 2972 m, 1485 s, 1456 s, 1368 s, 1185 s, 1115 s, 945, 914, vs, υ(Mo=O), 772 s, 752 vs, 712 s. ^{1}H NMR (CH_3CN-d_3, 400 MHz, r.t., δ (ppm)): 8.42 (s, 2H), 7.55–7.30 (m, 8H), 234 (s, 6H).

*4.8. MoO_2Br_2(o-phenyl-DAB) (**8**)*

A solution of $MoO_2Br_2(NC\text{-}Me)_2$ (1.22 g, 3.29 mmol) in THF (15 ml), was treated with *o*-phenyl-DAB (0.78 g, 3.29 mmol). The initial greenish colour of the solution changed immediately to orange. The reaction was stirred for 15 min and the solution was then concentrated to ca. 2 ml. An orange solid was precipitated by

addition of Et_2O and the solid was dried under vacuum. Yield: 90%.

$C_{16}H_{16}N_2O_2Br_2Mo$ (524.07): calcd. C 36.67, H 3.08, N 5.35; found C 36.70, H 3.23, N 5.32. IR (KBr, υ (cm^{-1})): 3057 w, 2958 w, 1485 m, 13371 s, 11,220 m, 939, 909, vs, υ(Mo=O), 768 s, 712 m. ^1H NMR ($CHCl_3$-d_1, 300 MHz, r.t., δ (ppm)): 8.46 (s, 2H), 7.82–7.34 (m, 8H), 2.51 (s, 6H).

4.9. MoO_2Cl_2(p-phenyl-DAB) (**9**)

A solution of $MoO_2Cl_2(THF)_2$ (0.62 g, 1.81 mmol) in THF (15 ml), was treated with *o*-phenyl-DAB (0.43 g, 1.81 mmol). The colour of the solution changed immediately to bright yellow and the reaction was stirred for further 15 min. The solution was then taken to dryness to yield a yellowish/red product, which was washed with diethyl ether and dried under vacuum. Yield: 97%.

$C_{16}H_{16}N_2O_2Cl_2Mo$ (435.16): calcd. C 44.16, H 3.71, N 6.44; found C 44.37, H 3.80, N 6.52. IR (KBr, υ (cm^{-1})): 3017 m, 2976 m, 1597 s, 1501 vs, 1371 vs, 1213 s, 1179 s, 945, 912, vs, υ(Mo=O), 856 s, 814 vs, 552 s, 519 s. ^1H NMR ($CHCl_3$-d_1, 300 MHz, r.t., δ (ppm)): 8.28 (s, 2H), 7.58–7.31 (m, 8H), 2.40 (s, 6H).

4.10. MoO_2Br_2(p-phenyl-DAB) (**10**)

A solution of $MoO_2Br_2(NC\text{-}Me)_2$ (0.71 g, 1.92 mmol) in THF (15 ml), was treated with *p*-phenyl-DAB (0.45 g, 1.92 mmol). The colour of the solution changed to orange and the reaction was allowed to stir for an additional 15 min. The solution was then concentrated to ca. 2 ml and a red solid was precipitated by addition of diethyl ether. The product was filtered off, washed with diethyl ether and dried under vacuum. Yield: 90%.

$C_{16}H_{16}N_2O_2Br_2Mo$ (524.07): calcd. C 36.67, H 3.08, N 5.35; found C 36.91, H 3.25, N 5.62. IR (KBr, υ (cm^{-1})): 3020 m, 2969 m, 2922 m, 1501 s, 13770 s, 1211 m, 941, 909, vs, υ(Mo=O), 812 vs, 519 m. ^1H NMR ($CHCl_3$-d_1, 300 MHz, r.t., δ (ppm)): 8.30 (s, 2H), 7.62–7.31 (m, 8H), 2.41 (s, 6H).

4.11. MoO_2Cl_2(Me-CYDAB) (**13**)

A solution of $MoO_2Cl_2(THF)_2$ (1.20 g, 3.50 mmol) in THF (15 ml), was treated with Me-CYDAB (0.87 g, 3.50 mmol). The colour of the solution changed immediately to pinkish red and the turbid solution was stirred for further 15 min. After concentration to ca. 3 ml. A pinkish red solid was precipitated by addition of diethyl ether. The product was washed with diethyl ether and dried under vacuum. Yield: 90%.

$C_{16}H_{28}N_2O_2Cl_2Mo$ (447.26): calcd. C 42.97, H 6.31, N 6.26; found C 43.13, H 6.35, N 6.34. IR (KBr, υ (cm^{-1})): 2926 vs, 2857 s, 1586 m, 1454 m, 1366 m, 1173 m, 1069 w, 939, 910, vs, υ(Mo=O), 839 w, 802 w. ^1H NMR ($CHCl_3$-d_1, 300 MHz, r.t., δ (ppm)): 4.08 (TT, 2H), 2.66–1.32 (m, 20H), 2.42 (s, 6H).

4.12. MoO_2Br_2(Me-CYDAB) (**14**)

A solution of $MoO_2Br_2(NC\text{-}Me)_2$ (0.89 g, 2.40 mmol) in THF (15 ml), was treated with Me-CYDAB (0.60 g, 2.40 mmol). The greenish solution changed to a brownish colour and the reaction was stirred for further 20 min. The turbid solution was then taken to dryness, the remaining pale brown solid was washed with cold CH_2Cl_2 and diethyl ether and the resulting white powder was dried under vacuum. Yield: 80%.

$C_{16}H_{28}N_2O_2Br_2Mo$ (536.16): calcd. C 35.84, H 5.2, N 5.22; found C 35.92, H 5.41, N 5.08. IR (KBr, υ (cm^{-1})): 2930 vs, 2857 s, 1578 w, 1454 m, 1397 w, 1366 m, 1171 m, 937, 909, υ(Mo=O), 802 w. ^1H NMR ($CHCl_3$-d_1, 300 MHz, r.t., δ (ppm)): 4.20 (TT, 2H), 2.63–1.31 (m, 20H), 2.43 (s, 6H).

4.13. MoO_2Cl_2(CYDAB) (**15**)

A solution of $MoO_2Cl_2(THF)_2$(1.21 g, 3.52 mmol) in THF (15 ml), was treated with

CYDAB (0.78 g, 3.52 mmol). A white precipitate was immediately formed and the reaction mixture was stirred for an additional 15 min. After concentration to ca. 4 ml and addition of diethyl ether, the solid was filtered off and the white powder was washed with diethyl ether and dried in oil pump vacuum. Yield: 98%.

$C_{14}H_{24}N_2O_2Cl_2Mo$ (416.21): calcd. C 40.11, H 5.77, N 6.68; found C 39.97, H 5.80, N 6.50. IR (KBr, υ (cm^{-1})): 2941 vs, 2914 vs, 2854 vs, 1448 vs, 1404 vs, 1352 vs, 1076 vs, 931, 912, vs, υ(Mo=O), 881 vs, 632 s. ^{1}H NMR (CH_3CN-d_3, 400 MHz, r.t., δ (ppm)): 8.22 (s, 2H), 4.17 (TT, 2H), 2.13–1.24 (m, 20H).

4.14. MoO_2Br_2(CYDAB) (16)

A solution of MoO_2Br_2(NC-Me)$_2$ (0.89 g, 2.40 mmol) in THF (15 ml), was treated with CYDAB (0.53 g, 2.40 mmol). A yellow/greenish turbid solution was formed and the mixture reaction was stirred for 30 min. After concentration to ca. 3 ml, a pale green solid was precipitated by addition of diethyl ether. The solid was filtered off, washed with diethyl ether and dried under vacuum. Yield: 98%.

$C_{12}H_{24}N_2O_2Br_2Mo$ (508.11): calcd. C 33.0, H 4.76, N 5.51; found C 33.50, H 4.84, N 5.57. IR (KBr, υ (cm^{-1})): 2942 vs, 2853 vs, 1449 vs, 1404 s, 1352 s, 1072 s, 930, 909, vs, υ(Mo=O), 880 s. ^{1}H NMR (CH_3CN-d_3, 400 MHz, r.t., δ (ppm)): 8.27 (s, 2H), 4.28 (TT, 2H), 2.22–1.25 (m, 20H).

4.15. MoO_2Cl_2(^{t}Bu-DAB) (17)

A solution of MoO_2Cl_2(THF)$_2$ (1.35 g, 4.20 mmol) in THF (15 ml), was treated with ^{t}Bu-DAB (0.71 g, 4.20 mmol). The colourless solution which formed was stirred for 15 min. The solution was then concentrated and then a white solid was precipitated by addition of diethyl ether. The product was filtered off, washed with diethyl ether and dried under vacuum. Yield: 90%.

$C_{10}H_{20}N_2O_2Cl_2Mo$ (367.13): calcd. C 32.72, H 5.49, N 7.63; found C 32.90, H 5.71, N 7.52. IR (KBr, υ (cm^{-1})): 2980 s, 2936 m, 1478 m, 1454 m, 1389 s, 1366 s, 1238 m, 1186 s, 1038 w, 968 s, 949, 912, vs, υ(Mo=O), 864 s, 758 m. ^{1}H NMR ($CHCl_3$-d_1, 300 MHz, r.t., δ (ppm)): 8.03 (s, 2H), 1.58 (s, 18H).

4.16. MoO_2Br_2(^{t}Bu-DAB) (18)

A solution of MoO_2Br_2(NC-Me)$_2$ (0.33 g, 0.90 mmol) in THF (15 ml), was treated with ^{t}Bu-DAB (0.15 g, 0.90 mmol). The colour of the solution changed immediately to yellow/green and was stirred for further 15 min. The solution was then concentrated to ca. 2 ml and the addition of diethyl ether precipitated a pale green product. The product was filtered off and dried under vacuum. Yield: 90%.

$C_{10}H_{20}N_2O_2Br_2Mo$ (456.03): calcd. C 26.34, H 4.42, N 6.14; found C 25.97, H 4.37, N 5.89. IR (KBr, υ (cm^{-1})): 2976 vs, 2934 s, 1478 s, 1389 vs, 1388 s, 1236 s, 1192 vs, 970 s, 943, 910, vs, υ(Mo=O), 866 s, 58 m. ^{1}H NMR ($CHCl_3$-d_1, 300 MHz, r.t., δ (ppm)): 8.05 (s, 2H), 1.57 (s, 18H).

4.17. MoO_2Cl_2(^{i}prop-DAB) (19)

A solution of MoO_2Cl_2(THF)$_2$ (0.58 g, 1.68 mmol) in THF (15 ml), was treated with ^{i}prop-DAB (0.24 g, 1.68 mmol). The colourless solution was stirred for 15 min, and after concentration and addition of diethyl ether, a white product was precipitated. The solid was filtered off, washed with diethyl ether and dried under vacuum. Yield: 95%.

$C_8H_{16}N_2O_2Cl_2Mo$ (339.07): calcd. C 28.34, H 4.76, N 8.24; found C 28.30, H 4.93, N 8.26. IR (KBr, υ (cm^{-1})): 2940 vs, 2853 vs, 1447 vs, 1402 s, 1352 m, 1072 s, 932, 909, vs, n(Mo=O), 880 s, 630 w. ^{1}H NMR ($CHCl_3$-d_1, 300 MHz, r.t., δ (ppm)): 8.21 (s, 2H), 4.70 (m, 2H), 1.63 (d, 12H).

4.18. $MoO_2Br_2(^i$prop-DAB) (20)

A solution of MoO_2Br_2(NC-Me)$_2$ (0.33 g, 0.90 mmol) in THF (15 ml), was treated with ^{i}prop-DAB (0.13 g, 0.90 mmol). The greenish solution changed immediately to a light yellow and was stirred for 15 min. The solution was then concentrated to ca. 2 ml and the addition of diethyl ether precipitated a yellow solid, which was washed with diethyl ether and dried under vacuum. Yield: 95%.

$C_8H_{16}N_2O_2Br_2Mo$ (427.98): calcd. C 22.45, H 3.77, N 6.55; found C 22.35, H 3.81, N 6.47. IR (KBr, υ (cm^{-1})): 2982 s, 2930 s, 1458 s, 1406 vs, 1368 s, 1329 s, 1149 s, 1127 vs, 941, 907, vs, υ(Mo=O), 831 s. ^{1}H NMR ($CHCl_3$-d_1, 300 MHz, r.t., δ (ppm)): 8.20 (s, 2H), 4.74 (m, 2H), 1.68 (d, 12H).

4.19. X-ray crystallography

Suitable single crystals for the X-ray diffraction studies were grown by standard techniques from saturated solutions. Both structures were solved by a combination of direct methods, difference-Fourier syntheses and full-matrix least-squares refinements. Neutral atom scattering factors for all atoms and anomalous dispersion corrections for the non-hydrogen atoms were taken from *International Tables for X-Ray Crystallography* [39]. All calculations were performed on a DEC 3000 AXP workstation with the *STRUX-V* [40] system, including the programs *PLATON-92* [41], *PLUTON-92* [41], *Sir-92* [42], and *SHELXL-93* [43].

4.20. Data collection, structure solution and refinement for the complexes (3 / 5 · $NCCH_3$)

Preliminary examinations and data collections were carried out on an imaging plate diffraction system (IPDS; STOE&CIE) equipped with a rotating anode (NONIUS FR591; 50/50 kV; 80/80 mA; 4.0/4.0 kW) and graphite monochromated MoK_α radiation. Data collections were performed at 193 K within the Θ-range of 2.73° to 24.81/3.68° to 30.38° with an exposure time of 150/60 s per image (oscillation scan modus from $\phi = 0.0°$ to 360° with $\Delta\phi = 1°$). A total number of 10,624/39,186 reflections were collected. 216/850 systematic absent reflections 237/1519 negative intensities together with 0/6156 very weak intensities with $\Theta > 28.00°$ were rejected from the original data set. After merging a sum of 1473/4448, independent reflections remained and were used for all calculations. Data were corrected for Lorentz and polarization effects. Corrections for absorption and decay effects were applied with the program DECAY [44]. The unit cell parameters were obtained by full-matrix least-squares refinements of 1882/1976 reflections with the program CELL [44]. All ''heavy atoms'' of the asymmetric unit were anisotropically refined. Hydrogen atoms were found in the difference maps and refined with individual isotropic thermal displacement parameters. For compound **5** · $NCCH_3$ the hydrogen atoms of the disordered solvent acetonitrile were placed in calculated positions. Full-matrix least-squares refinements were carried out by minimizing $\Sigma w(F_o^2 - F_c^2)^2$ with *SHELXL-93* weighting scheme and stopped at shift/err < 0.006/0.001.

Crystallographic data (excluding structure factors) for the structures reported in this paper have been deposited with the Cambridge Crystallographic data center as supplementary publication no. CCDC-103338 and CCDC-103339. Copies of the data can be obtained free of charge on application to CCDC, 12 Union Road, Cambridge CB2 1EZ, UK [Fax: int. code +44(1223)336-033; E-mail: deposit @ccd.cam.ac.uk].

4.21. Catalytic reactions with compounds 1–20 as catalysts

800 mg (7.3 mmol) *cis*-cyclooctene, 800 mg *n*-dibutylether (internal standard), 1 mol% (73 μmol) **1**–**20** (as catalyst), and 2 ml 5.5 M *tert*-butylhydroperoxide in decane were added to a thermostated reaction vessel and stirred for 4 h at 55°C.

The course of the reaction was monitored by quantitative GC-analysis. Samples were taken every 30 min, diluted with chloroform, and chilled in an icebath. For the destruction of hydroperoxide and removal of water, a catalytic amount of manganese dioxide and magnesium sulfate was added. After the gas evolution ceased, the resulting slurry was filtered over a filter equipped Pasteur pipette and the filtrate injected in the GC column.

The conversion of cyclooctene and formation of cyclooctene oxide was calculated from a calibration curve ($r^2 = 0.999$) recorded prior to the reaction course.

Acknowledgements

This work was supported by PRAXIS XXI, Project (2/2.1/QUI/419/94). The authors want to thank the DAAD and CRUP (INIDA and Acções Integradas Programme) for generous support. A.D.L. thanks PRAXIS XXI, A.M.S. thanks the Bayerische Forschungsstiftung for a grant. The authors greatly acknowledge Prof. W.A. Herrmann for generous support.

References

[1] R.A. Sheldon, J. Mol. Catal. 7 (1980) 107.
[2] W.R. Thiel, T. Priermeier, Angew. Chem., Int. Ed. Engl. 34 (1995) 1737.
[3] W.R. Thiel, J. Mol. Catal. 117 (1997) 449.
[4] W.R. Thiel, J. Eppinger, Chem. Eur. J. 3 (1997) 696.
[5] F.P. Ballisteri, G.A. Tomaselli, R.M. Toscano, V. Conte, F. di Furia, J. Mol. Catal. 89 (1994) 295.
[6] S. Campestrini, F. di Furia, J. Mol. Catal. 79 (1993) 13.
[7] N. Indictor, W.F. Brill, J. Org. Chem. 29 (1965) 2075.
[8] U.S. Patent No. 3.350.422, 1967.
[9] U.S. Patent No. 3.351.635, 1967.
[10] U.S. Patent No. 3.507.809, 1970.
[11] U.S. Patent No. 3.625.891, 1971.
[12] D.D. Agarwal, Inorg. Chem. 25 (1986) 65.
[13] E.P. Talsi, K.V. Shalyaev, K.I. Zamaraev, J. Mol. Catal. 83 (1993) 347.
[14] R.H. Holm, Chem. Rev. 87 (1987) 1401.
[15] L.R. Florian, E.G. Corey, Inorg. Chem. 7 (1968) 722.
[16] B. Spivack, Z. Dori, Coord. Chem. Rev. 17 (1975) 99.
[17] F. Trifiro, P. Forzatti, S. Preite, I. Pasquon, J. Less-Common Met. 36 (1974) 319.
[18] P. Chaumette, H. Mimoun, L. Saussine, J. Fischer, A. Mitschler, J. Organomet. Chem. 250 (1983) 291.
[19] F.E. Kühn, E. Herdtweck, J.J. Haider, W.A. Herrmann, I.S. Gonçalves, A.D. Lopes, C.C. Romão, J. Organomet. Chem. 583 (1999) 3.
[20] K. Dreisch, C. Andersson, C. Stalhandske, Polyhedron 12 (1993) 303.
[21] H. Arzoumanian, G. Agrifoglio, H. Krentzien, M. Capparelli, J. Chem. Soc., Chem. Commun. (1995) 655.
[22] D.M. Baird, F.L. Yang, D.J. Kavanaugh, G. Finess, K.R. Dunbar, Polyhedron 15 (1996) 2597.
[23] M. Minelli, J.H. Enemark, R.T.C. Brownlee, M.J. O'Connor, A.G. Wedd, Coord. Chem. Rev. 68 (1985) 169.
[24] S. Berger, S. Braun, H.C. Kalinowski, NMR-Spektroskopie von Nichtmetallen, Vol. 1, Georg Thieme Verlag, Stuttgart, 1992.
[25] W.A. Herrmann, F.E. Kühn, P.W. Roesky, J. Organomet. Chem 485 (1995) 243.
[26] W.A. Herrmann, F.E. Kühn, M.U. Rauch, J.D.G. Correia, G. Artus, Inorg. Chem. 34 (1995) 2914.
[27] C.C. Romão, F.E. Kühn, W.A. Herrmann, Chem. Rev. 97 (1997) 3197.
[28] F.A. Cotton, R.M. Wing, Inorg. Chem. 4 (1965) 867.
[29] F.H. Allen, O. Kennard, 3D search and research using the Cambridge structural database, Chemical Design Automation News 8 (1993) 1 and 31.
[30] W.A. Herrmann et al., personal communication.
[31] F.E. Kühn, A.D. Lopes, I.S. Gonçalves, A.M. Santos, E. Herdtweck, C.C. Romão, submitted for publication.
[32] H. Iida, Y. Yuasa, C. Kibayashi, Y. Iitaka, J. Chem. Soc. Dalton Trans. (1956) 640.
[33] H.F. Holtzclaw, J.P. Coleman Jr., R.M. Alire, J. Am. Chem. Soc. 80 (1958) 1100.
[34] P. Kiprof, W.A. Herrmann, F.E. Kühn, W. Scherer, M. Kleine, M. Elison, K. Rypdal, H.V. Volden, S. Gundersen, A. Haaland, Bull. Soc. Chim. Fr. 129 (1992) 655.
[35] G. van Koten, K. Vrieze, Advances in Organometallic Chemistry, Vol. 21, Academic Press, New York, 1982.
[36] R. Colton, I.B. Tomkins, Aust. J. Chem. 18 (1965) 447.
[37] H.L. Kraus, W. Huber, Chem. Ber. 94 (1961) 2864.
[38] W.M. Carmichael, D.A. Edwards, G.W.A. Fowles, P.R. Marshall, Inorg. Chim. Acta 1 (1967) 93.
[39] International Tables for Crystallography, Vol. C, Tables 6.1.1.4 (pp. 500–502), 4.2.6.8 (pp. 219–222), and 4.2.4.2 (pp. 193–199), in: A.J.C. Wilson (Ed.), Kluwer Academic Publishers, Dordrecht, The Netherlands, 1992.
[40] G.R.J. Artus, W. Scherer, T. Priermeier, E. Herdtweck, S T R U X–V, A Program System to Handle X-ray Data, TU München, Germany, 1997.
[41] A.L. Spek, PLATON-92–PLUTON-92, an integrated tool for the analysis of the results of a single crystal structure determination, Acta Crystallogr., Sect. A 46 (1990) C34.
[42] G. Cascarano, C. Giacovazzo, A. Guagliardi, M.C. Burla, G. Polidori, M. Camalli, SIR-92, University Bari, Italy, 1992.
[43] G.M. Sheldrick, SHELXL-93, in: G.M. Sheldrick, C. Krüger, R. Goddard (Eds.), Crystallographic Computing 3, Oxford Univ. Press, England, 1993, pp. 175–189.
[44] IPDS Operating System Version 2.8 STOE&CIE., Darmstadt, Deutschland, 1997.